Received: 27 June 2022 | Revised: 9 September 2022 | Accepted: 11 September 2022

DOI: 10.1002/pen.26150

RESEARCH ARTICLE

POLYMER ENGINEERING AND SCIENCE WILEY

Bilayer biocomposites of PVOH/WPI/nano-silica treated with corona discharge

Bruna Rage Baldone Lara[1] | **Paulo Sérgio de Andrade**[1] | **Ana Carolina Salgado de Oliveira**[1] | **Mario Guimarães Junior**[2] | **Lays Camila Matos**[3] | **Gustavo Henrique Denzin Tonoli**[3] | **Marali Vilela Dias**[1]

[1]UFLA/Department of Food Science, Federal University of Lavras, Lavras, Brazil

[2]CEFET-MG/Department of Electromechanics, Federal Center of Technological Education of Minas Gerais, Araxa, Brazil

[3]UFLA/Department of Forest Science, Federal University of Lavras, Lavras, Brazil

Correspondence
Ana Carolina Salgado de Oliveira, UFLA, Federal University of Lavras, University Campus, PO Box: 3037, CEP: 37200-900, Lavras, MG, Brazil.
Email: anacarolengalimentos@gmail.com

Funding information
Conselho Nacional de Desenvolvimento Científico e Tecnológico; Coordenação de Aperfeiçoamento de Pessoal de Nível Superior; Fundação de Amparo à Pesquisa do Estado de Minas Gerais

Abstract

In order to evaluate the influence of a different assembly of biocomposites of polyvinyl alcohol (PVOH), whey protein isolates (WPI), and nano-silica (NS), a bilayer film treated with corona discharge was produced through a two-step lamination. The first layer of PVOH/NS, treated with up to 90 s of discharge, and the second layer of WPI/NS, the bilayer films had their morphology, tensile strength, and water barrier investigated and compared to a single layer PVOH/WPI/NS film. Corona discharge increased the wettability of the first layer, improving the ability to interact with the second layer, thus increasing the adherence between these layers. Films treated with higher times of discharge showed a homogeneous transition between phases, suggesting compatibility, and adherence between layers. At 90 s of corona discharge treatment, bilayer films showed a tensile strength 72% higher than the bilayer film not treated and also 23% more resistant and 7.4 times more ductile than the single-layer film. The lamination process and corona treatment increase the affinity of water with film constituents, thus leading to a higher permeability. The use of corona discharge associated with the lamination of PVOH/WPI/NS biocomposites provides a bilayer film and produces a more resistant, flexible, and ductile biocomposite film for packaging.

KEYWORDS

bilayer packaging film, biocomposite, Corona discharge, nano-silica, polyvinyl alcohol, whey protein isolate

1 | INTRODUCTION

One of the biggest markets for plastics is that of packaging, which is projected to grow at a compound annual growth rate of 4.2% from 2021 to 2026, being polyethylene and polypropylene are the major raw materials used for packaging applications.[1,2] The high interest in biodegradable films as an alternative to these non-biodegradable petroleum-based film packaging is confirmed by the compound annual growth rate of 17.1% expected for the market of bioplastics from 2021 to 2028. In this context, more research related to the use of renewable proteins as biopolymers in the food packaging sector has been performed.[3]

Whey protein isolate (WPI) films have desirable film-forming and excellent gas barrier properties when compared to petroleum-based synthetic films, but present low tensile strength and intrinsic stiffness.[4–6] Among the

numerous methods proposed to overcome these inherent shortcomings of WPI films, it is possible to cite: blending with other biodegradable polymers, coating, lamination, plasticization, nanomaterial adding, and cross-linking, for example. Polyvinyl alcohol (PVOH) is one polymer that has attracted huge attention due to its high optical clarity, mechanical stability, biodegradability, environmental-friendly fabrication process, and compatibility with many compounds. In previous works, it was proved that the addition of PVOH and colloidal nano-silica (NS) to the WPI matrix was effective in improving flexibility, strongly reducing stiffness, and also increasing the tensile strength of the WPI matrix.[3,7,8] In order to improve even more these tensile mechanical properties, a new assembly of the WPI/PVOH/NS biocomposite is proposed in this work.

One still poorly explored way to manipulate the properties of the components is by developing bilayer films.[9] With this different assembly, guaranteeing good adherence between layers, a bilayer film can achieve different properties from those of a single-layer film composed of the same raw materials. In the present study, the adherence between layers was provided by a corona discharge treatment, which is a low-cost and sustainable surface modification technology frequently used by the packaging industry in order to increase the surface energy and polarity of films, thus improving wettability and adhesion properties.[10–12]

In this study, a novel-designed bilayer film was developed through a two-step lamination casting method, with the first layer of PVOH/NS treated by 0 to 90 s of corona discharge and the second layer of WPI/NS. A film control of PVOH/WPI/NS with a single layer was also produced seeking to evaluate the effect of corona discharge and lamination on the tensile and water barrier properties of the biocomposites evaluated by tensile, permeability, and diffusion tests. The first layer was characterized by the water contact angle, surface energy, and Fourier transform infrared (FT-IR) analysis in order to understand the changes provided by the different times of corona discharge. The morphology of the joining region between layers was evaluated through Scanning Electron Microscopy (SEM) micrographs. This study provides a worthwhile way for designing a novel bilayer PVOH/WPI/NS biocomposite with the desired tensile properties.

2 | MATERIAL AND METHODS

2.1 | Material

Polyvinyl alcohol with high molecular weight (Mw = 130.000 $g.mol^{-1}$) and highly hydrolyzed (99%), from Sigma-Aldrich; whey protein isolate (WPI 9400) with 90% of proteins, from Hilmar Ingredients; glutaraldehyde solution (25% in H_2O), as PVOH crosslinking agent, from Sigma-Aldrich[13,14]; glycerol (≥ 99.5%, density 1.26 $g.mL^{-1}$), as a plasticizing agent, produced by Sigma-Aldrich; granulated anhydrous citric acid from Cargill Agrícola S.A was used to guarantee a good distribution of NS[3]; and NS from colloidal solution Bindzil 2034DI (Akzo Nobel), with 34% in weight of NS (average particle size of 15 nm and 200 m^2g^{-1} of surface area).

2.2 | Experimental design and preparation of the biocomposites

This research was performed in two phases: the first one with the production of the first layer film of PVOH/NS, applying different periods of corona discharge (0, 30, 60, and 90 s) and evaluating the first layer exactly after the discharge through water contact angle, surface energy, and FT-IR analysis; and the second phase, with the production of the bilayer films (the first layer of PVOH/NS treated with the cited different periods of corona and the second layer of WPI/NS applied right after the discharge), which were analyzed through SEM, tensile, and water barrier tests. The scheme shown in Figure 1 explains clearly the experimental design.

2.2.1 | Bilayer biocomposites

Crosslinked PVOH/NS—first layer

The PVOH solution was prepared using a polymer concentration of 6% $m.v^{-1}$ and adding 30% of glycerol (m. m^{-1} of polymer) and 8% of citric acid (m/m of polymer). The solution was agitated for 30 min (250 rpm) and conducted in a water bath at 90°C for 1 h until complete PVOH solubilization. After being cooled at room temperature, NS (Bindzil 2034DI) was added to the solution at 4% m/m of polymer (4 g of NS was added for each 100 g of PVOH). The final solution was homogenized in Ultra Turrax (Kika Labortchnik) for 20 min (450 rpm) and after sonified (Sonifier Cell Disruptor Branson—Model 450D, Manchester, UK) using a probe with 100 mm of diameter, at 60% of amplitude (270 W), for 10 min (600 s) in a continuous assay, using an ice bath to avoid heating, resulting in ultrasonic energy applied of 810 J. mL^{-1}. The sonicated solution was then crosslinked by adding 5% ($m.m^{-1}$ of polymer) of glutaraldehyde and agitated for 15 min at 250 rpm. Final solutions were shed on circular acrylic plates (707 cm^2), perfectly leveled, and conditioned at room temperature (25°C) for spontaneous drying (48 h). The dried films were conditioned under controlled temperature and relative

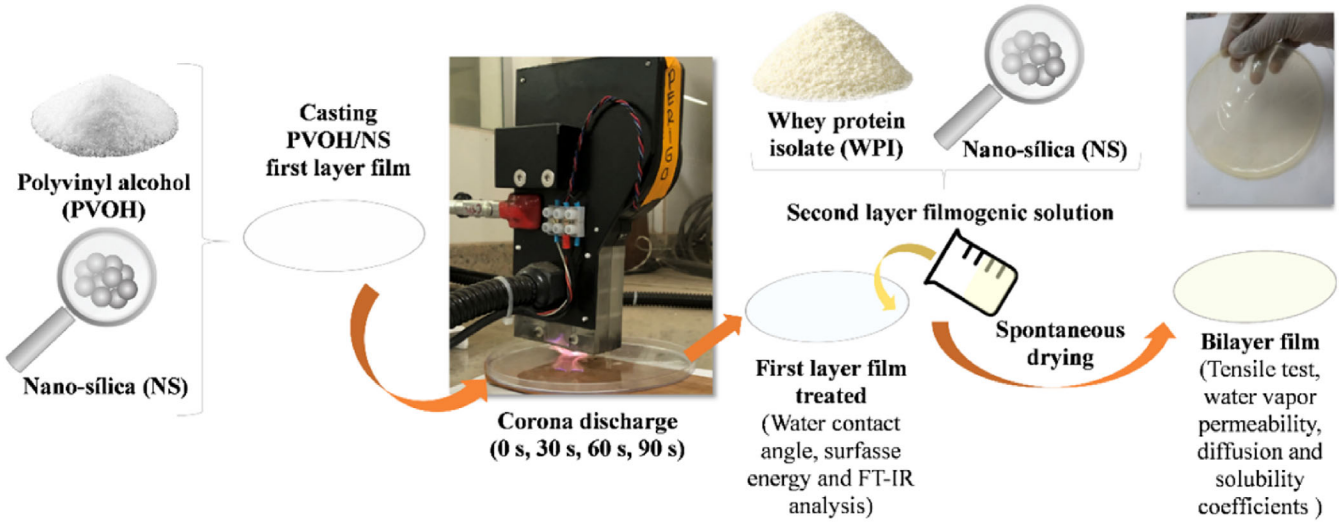

FIGURE 1 Experimental design of preparation and tests of the biocomposites

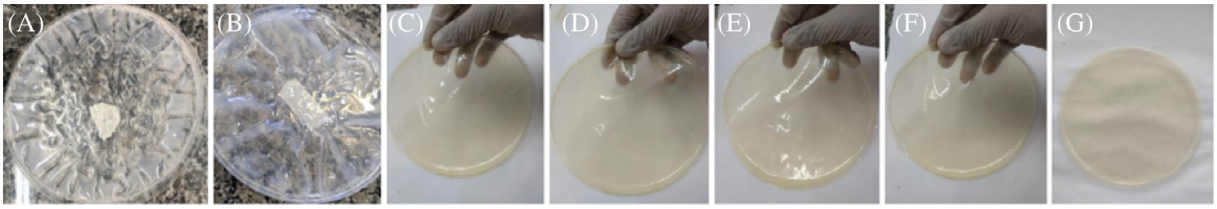

FIGURE 2 Photos of tests and biocomposite films produced (A) test with WPI solution as the first layer and PVOH as the second layer; (B) test with PVOH not crosslinked as the first layer and WPI as the second layer; (C) B0S; (D) B30S; (E) B60S; (F) B90S; and (G) UNL

humidity (RH) (25 ± 1°C and 50% RH) for 48 h before corona treatment.

PVOH crosslinked with glutaraldehyde was chosen as the first layer since, in previous tests, WPI or PVOH crosslinked films as first layers were not water-resistant enough to receive the second layer solution, solubilizing as shown in Figures 2A,B.

Samples of the first layer films (of PVOH and nano-silica, crosslinked with glutaraldehyde) were then submitted to the corona discharge, using Corona Brasil equipment (model PT) with a power of 0.5 kW, a discharge of 10 kV, an intensity of 60 μA, a frequency of 60 Hz, and an air-gap between the electrode and the sample film set at 15 mm. Four different treatments were produced, varying the period of corona discharge: 0, 30, 60, and 90 s, corresponding, respectively, to the 0S, 30S, 60S, and 90S treatments. Three replicates of each treatment were performed.

WPI/NS—Second layer

The WPI solution was prepared using a concentration of 6% m/v, added with glycerol (30% m/m of WPI), citric acid (8% m/m of WPI), and kept under agitation for 30 min (250 rpm) at room temperature (25°C). The solution had the pH adjusted to 8 using a NaOH solution (3 M) and was then submitted to a water bath at 90°C for 30 min to guarantee protein denaturation.[15] After cooled at room temperature, nano-silica, NS, (Bindzil 2034DI) was added at 4% m/m of polymer (4 g of NS was added for each 100 g of WPI), and the solution was homogenized in Ultra Turrax, following the same conditions used for the PVOH/NS first layer solution.

Final solutions were shed on top of the first-layer films of PVOH and nano-silica and conditioned at room temperature (25°C) for spontaneous drying (48 h). The dried bilayer biocomposites treated with corona discharge at 0 s, 30 s, 60 s, and 90 s were, respectively, named B0S, B30S, B60S, and B90S, and conditioned under controlled temperature and relative humidity (RH) (25 ± 1°C and 50% RH ±2%) for 48 h before characterization. Photos of the bilayer films produced are shown in Figure 2C–F.

2.2.2 | Unlaminated film

The unlaminated biocomposite film (UNL), with a single layer, was prepared following the same procedures from 3. WPI and PVOH solutions were separately prepared

using a polymer concentration of 6% m.v-1 and adding 30% of glycerol (m.m-1 of polymer), and 8% of citric acid (m/m of polymer). Both solutions were agitated (30 min, 250 rpm, at a room temperature of 25°C) and conducted in the water bath at 90°C (WPI solution for 30 min and PVOH solution for 60 min of bath). WPI and PVOH solutions were merged in a volumetric proportion of 70/30 and, after cooling at room temperature, nano-silica (Bindzil 2034DI) was added to 4% m/m of polymer. The final solution was homogenized in Ultra Turrax, sonified, shed circular acrylic plates, dried, and conditioned under the same conditions as those from the first and second layer of the bilayer films. A photo of the unlaminated film produced is shown in Figure 2G.

2.3 | Characterization of the biocomposites

2.3.1 | First layer characterization

Exactly after the corona discharge, the film solution of the second layer (WPI and nano-silica) was shed on top of the first layers treated. Besides that, at a maximum time of 20 minutes after the corona discharge, samples of each treatment (0S, 30S, 60S, and 90S) were submitted to FT-IR, contact angle, and surface energy analysis to understand the surface modifications caused by the discharge.

Determination of the water contact angle and surface energy

The water contact angle measurement was performed to understand the modifications caused by the different times of corona discharge at the first layer film surface wettability. For this purpose, it was used the sessile drop method and a Goniometer (KRUSS, Drop Shape Analyzer-DSA25) in which, through a syringe, a drop of the standard liquid was applied to the surface to be characterized.[16–22] The static angle between the drop and the biocomposite surface was calculated through the slope of the tangent. The average of the left and right angles was obtained as the final value of the contact angle.

The contact angle analysis was performed by fixing biocomposite samples on glass slides and attaching them to the equipment. A drop of the liquid was placed on the biocomposite surface and the goniometer carried out 10 angle measurements per second for 2 s.[23] To determine the wettability, distilled water was used, while for surface energy, besides the distilled water, ethylene glycol and methane diode were used as well. Images of the drop at the film surface for each treatment were also captured by the equipment, and the average angle was indicated.

The dispersion of surface energy was calculated following the procedure described by Owens-Wendt, considered universal for the calculation of surface energy, using two test liquids: water and diiodomethane.[22] The existing relationship for surface energy was extended and the hydrogen bonds added in the non-dispersive component were renamed the polar component (p) (Equation 1).[24] It was assumed that the interaction between two materials is also a function of polar components and is described by a geometric mean, where only forces of the same nature interact (Equation 2).[24]

$$\gamma_i^T = \gamma_i^d + \gamma_i^p \quad (1)$$

$$\gamma_{i/j} = \gamma_i + \gamma_j - 2\left(\sqrt{\gamma_i^d + \gamma_j^d} + \sqrt{\gamma_i^p + \gamma_j^p}\right) \quad (2)$$

where γ is superficial free energy; γ^T is total surface free energy; d is the dispersive interactions; and p is the polar component.

Fourier transform infrared analysis

To understand the effects of the corona discharge at the surface, the first layer film samples were characterized by absorption spectroscopy in the region of infrared through an FTS 3000 Excalibur Digilab (United States), in Total Attenuated Reflection mode, equipped with a KBr detector. The analysis range was from 4000 to 400 cm^{-1} with 64 scans.

2.3.2 | Bilayer and unlaminated biocomposite characterization

Scanning electron microscopy

SEM micrographs were obtained to evaluate the biocomposite morphology at the joining region of the two layers, looking for flaws, phase separation, or any other effect that could be related to the mechanical and water barrier results. The analysis was conducted on an LEO 1430 VP (England) with an accelerating voltage of 20 kV, obtaining microscopies with 1000X magnification. To observe the morphology at the cross-section, the specimens were previously frozen in liquid nitrogen and fractured, and then gold (Au)-coated using vapor deposition.

Tensile properties

The tensile test was performed to verify the influence of lamination and corona discharge on the strength, flexibility, and ductility of the biocomposites when submitted to stretching stress. The maximum tensile strength (TS), the tensile modulus (TM), and the maximum elongation (E) of the biocomposites were measured according to,[25]

using a texturometer (Stable Microsystems, model TATX2i, England) with a load cell of 1 kN and a speed of 10 mm.s^{-1}. Specimens of 5 mm in width and 100 mm in length were tested at 23°C ± 1°C. TM was calculated through the tangent of the initial linear function of the stress–strain curve, which was considered an elastic behavior. By dividing the maximum tensile by the film transversal section area and by the percentage relationship between the final and initial length of the specimen, respectively, TS and E were obtained. Five repetitions were used for each replicate of the five different biocomposites. Thickness (mm) was measured using a digital micrometer (Digimess) with a resolution of 0.001 mm, taking five random measurements per specimen.

Water vapor permeability coefficient

Water vapor permeability coefficient (P) was determined by the gravimetric method, following the ASTM-E96/E96M[26] and using circular specimens of 80 mm in diameter. The specimens were fixed in circular capsules with 5.2 cm of effective permeation area. In the interior of capsules, it was added silica gel, set at low humidity, which was considered as 0 (zero) in the atmosphere in contact with the specimen's lower face.[8] The capsules were placed in hermetic desiccators at 25°C ± 1°C with a sodium chlorate saturated solution, setting the humidity to 75%. Weight gain measurements were taken by weighing the capsules (Analytical balance, resolution 0.001 g) every 24 h for 7 days. A plot of weight gained (*Wg*) versus time (*t*) was used to determine the WVP through Equation (3):

$$P = \frac{Wg \times ti}{t \times A \times \rho_s(\mathrm{RH}_1 - \mathrm{RH}_2)} \tag{3}$$

where *P* is given in g.cm.cm^{-2}.s^{-1}.kPa^{-1}; A is the permeation area of the specimen (cm^2); *ti* is the medium specimen thickness (cm); *ρs* is the water vapor saturation pressure at the test temperature (3169 kPa); RH_1 is the relative humidity of the desiccator chamber (0,75) and RH_2 (0,00) is the relative humidity inside the capsule. Three repetitions were performed for each biocomposite.

Determination of water diffusion and solubility coefficients

The effective diffusion coefficient (Deff) of water was determined using Fick's model for diffusion, shown in Equation (4), which can be simplified when considering that the water diffusion occurs in a unique direction, as expressed in Equation (5). Besides that, considering (i) a membrane with uniform thickness (ii) and surfaces, $x = -l$ and $x = l$, with a known constant concentration of water (C_0), and (iii) the concentration of water inside the film is zero, the diffusion equation can be expressed as Equation (6).[27] For short periods, Equation (3) can be simplified as shown in Equation (7), which can be used to adjust the initial experimental points, until 60% of the solute mass has been absorbed.[27]

$$\frac{\partial C}{\partial t} = D_{eff}\left(\frac{\partial^2 C}{\partial x^2} + \frac{\partial^2 C}{\partial y^2} + \frac{\partial^2 C}{\partial z^2}\right) \tag{4}$$

$$\frac{\partial C}{\partial t} = D_{eff}\left(\frac{\partial^2 C}{\partial x^2}\right) \tag{5}$$

$$\frac{M_t}{M_\infty} = 1 - \frac{8}{\pi^2}\sum_{N=0}^{\infty}\frac{1}{(2N+1)^2}\exp\left[\frac{-D_{eff}(2N+1)^2\pi^2 t}{e^2}\right] \tag{6}$$

$$\frac{M_t}{M_\infty}(\leq 0,60) = 4\sqrt{\frac{D_{eff}.t}{e^2\pi}} \tag{7}$$

where *C* is the water concentration (g.cm^{-3}), D_{eff} is the effective diffusion coefficient (cm^2.s^{-1}), *x*, *y* e *z* are the dimensions of the film with significant diffusivity (cm), x = thickness, y = 0, and z = 0 (when occurring in only one direction, x), M_t (g) is the total amount of diffusing substance that has entered the membrane at the time *t* (s), M_∞ (g) is the corresponding moisture amount after the infinite time (equilibrium moisture), *N* is the number of terms in the series and *e* is the thickness of the film (cm).

The experimental test was conducted by preparing specimens of 6 cm^2 in triplicate and submitting them to vacuum drying at 70°C for 24 h. The samples were placed in a hermetic pot with a relative humidity of 75% (saturated saline solution of NaCl) at 25°C in order to measure their moisture gain. All samples were weighted with an accuracy of 0.001 g from the time zero to equilibrium (approximately 8 days), in a 24 h interval. For the first 9 h, when there were significant changes in mass, weight was measured at each hour. Through the moisture gain by time data and considering the thickness of each sample, it was possible to estimate the value of D_{eff} through a non-linear regression with Equation (7) (using a number of terms of the series truncated to $N = 10$).

Besides the diffusivity coefficient, it is also important to know the solubility coefficient since the film's moisture permeability is influenced by both the penetration of water molecules into the material and the water molecule's solubility in the biocomposite matrix.[28] Considering the biocomposite as a finite solid, with a water vapor concentration-independent diffusion constant, where initially the film is free from vapor and one surface is then exposed to a pressure p_1, giving a concentration in the surface layer of c_1, the amount of water vapor *Q* diffusing through the material is with thickness *X* in a time *t* is[28]:

TABLE 1 Results of water contact angle (WCA), diiodo-methane contact angle (DCA), surface energy (SE), dispersive interactions energy (DE), and polar interactions energy (PE) for each first layer (PVOH/NS) film

Treatment	WCA (°)	SE ($N.m^{-1}$) × 10^{-3}	DE ($N.m^{-1}$) × 10^{-3}	PE ($N.m^{-1}$) × 10^{-3}
0S	105.92 ± 2.94[c]	27.96 ± 3.44	27.81 ± 3.53	0.15 ± 0.03
30S	41.08 ± 2.92[b]	59.87 ± 6.43	34.73 ± 3.80	25.14 ± 2.14
60S	29.55 ± 2.17[a]	67.42 ± 7.60	35.91 ± 4.12	31.5 ± 2.78
90S	27.00 ± 2.27[a]	70.48 ± 8.16	40.44 ± 5.41	31.04 ± 3.09

Note: In vertical columns, different letters represent significantly different values at ($p \geq 0.05$) using the Scott-Knott test.

$$Q = \frac{Dc_1 t}{X} - \frac{c_1 X}{6} \quad (8)$$

where D is the diffusion coefficient. The amount of water vapor permeating through the biocomposite increases linearly with time once the steady state has been reached. Considering a Fickian diffusion and sorption following Henry's law, at steady-state diffusion, it is possible to use the permeability coefficient (P) and the experimentally calculated diffusion coefficient (D_{eff}) to obtain the solubility coefficient through Equation (9)[28–30]:

$$S = P/D_{eff} \quad (9)$$

Is important to mention that, to obtain these P and S coefficients, four conditions were taken: (i) diffusion is at steady-state; (ii) the concentration–distance relationship through the biocomposite is linear; (iii) diffusion takes place only in one direction (through the biocomposite); and (iv) both D and S are not dependent on the concentration.[28] The application of these conditions to the considered materials is a simplification in order to obtain estimated values of P and S to better discuss the influence of corona treatment on the water permeation process.

2.4 | Statistical analysis

Sisvar 5.0 was used to perform a statistical analysis of the results by comparing the means through the Scott-Knott test with a 95% confidence level. The test was used for contact angle, tensile, water vapor permeability, water diffusion coefficient, and water solubility coefficient results.

3 | RESULTS AND DISCUSSION

3.1 | Water contact angle and surface energy

The contact angle was verified to measure the wettability changes in the PVOH/NS surface after the different times of corona treatment: a smaller contact angle means better wettability to receive the second layer of WPI/NS, which can be directly related to water permeation and tensile properties of the bilayer biocomposites (see Table 1).

The angle between the water drop and the biocomposite surface was decreased with the time of corona discharge increment, corroborating the ability of this treatment to increase the wettability of the surface. The WCA results can be visually understood in Figure 3. The film surface not treated by corona (0S) presented a hydrophobic surface, with a WCA higher than 90° (105.92°). Despite the fact that highly hydrolyzed PVOH is a polymer with a high affinity for water, it is understood that the insertion of 4% NS was able to make the film hydrophobic. This hydrophobic water contact angle was probably due to the ability of NS to fill the free volumes between PVOH chains, interacting with them through hydrogen bonds, as observed in previous work.[3] The more time the surface was treated with corona, the more the wettability of the WPI/NS film surface was increased. The lowest, and therefore, more hydrophilic angle was observed when the film surface was treated for the longest period of time, 90 s (27.00°). This result indicates that corona discharge improves the ability of the PVOH/NS surface to interact with the second layer of WPI/NS, increasing the adherence between these layers, which certainly influences the barrier and mechanical properties of the bilayer biocomposites.

The surface energy of the biocomposites was increased with the corona treatment, showing higher polar interactions energy and a slight increase in dispersion interactions energy. These results indicate that the discharge was able to improve the wettability of the PVOH/NS film surface. The film with 90 seconds of corona discharge (90S) showed surface energy 152% higher and polar energy 206 times higher than that with no corona discharge (0S). The reduction is in accordance with the water contact angle results, corroborating the hypotheses that the corona treatment is able to increase the adherence between the polymeric layers.

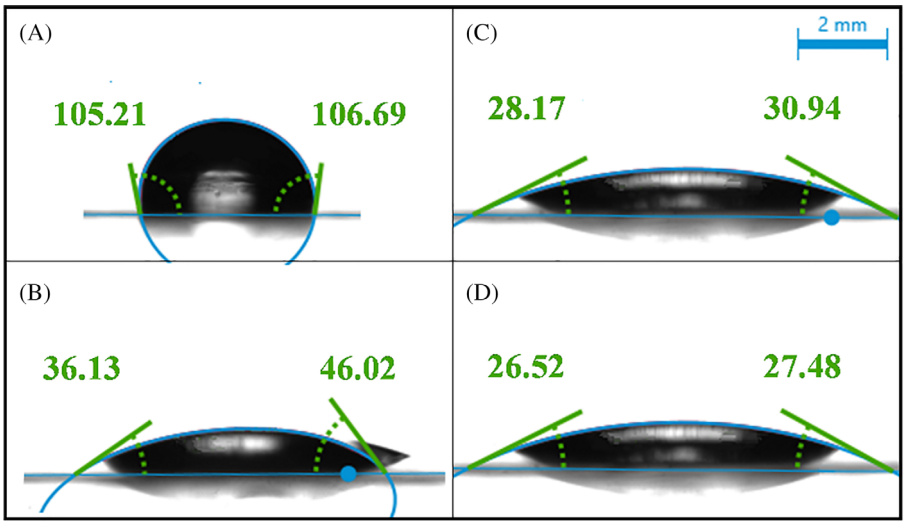

FIGURE 3 Water contact angles (right and left) formed between the water drop and the first layer films (A) 0S; (B) 30S; (C) 60S; and (D) 90S

3.2 | Fourier transform infrared analysis

The corona treatment leads to chemical and structural changes in surface area, generating reactive oxidants, such as ozone, oxygen-free radicals, or oxygen atoms, through electron bombardment at the surface.[11,31] As a result, the treatment provides the creation of carbonyl, carboxyl, hydroxyl, or ester functional groups at the polymer surface, which allows the increase of wettability. The groups formed at the PVOH/NS surface after corona discharge will be discussed with the results from FT-IR analysis.

Figure 4 presents spectra in the infrared region of PVOH/NS films after different times of corona discharge. The main absorptions occurred on bands: from 3600 to 2800 cm^{-1} and from 1800 to 950 cm^{-1}. These specific regions of the general spectra (Figure 3A) can be better observed in Figures 3B,C.

A broadband was observed for all treatments around 3260 cm^{-1} corresponding to de –OH stretching. It can be observed that the higher intensity of this band and a dislocation to lower wavenumbers for films treated with 60 and 90 s of corona discharge. This result indicates an increase in –OH groups and hydrogen bonds with the higher times of discharge.[3] The two peaks at 2940 cm^{-1} and 2910 cm^{-1} related to the asymmetrical and symmetrical stretching of methylene groups, respectively.[14]

Peaks at 1700 and 1650 cm^{-1} can be related to the axial deformation of carbonyl and/or ester groups, indicating their formation on the sample surface and contributing to the wettability increase.[32] At 1415 and 1325 cm^{-1} absorbance can be assigned to the $–CH_3$ bending.[30] An important change, which corroborates the generation of polar groups at the film surface after corona, is the disappearance of the peak at 1200 cm^{-1} (–C–O–C– stretching) and the reduction of the band intensity at 1085 cm^{-1} (–C–O– stretching) and 1040 cm^{-1} (–OH bending), with the subsequent new peak at 1235 cm^{-1} indicating the formation of carbonyl and/or ester groups.[30,32] Table 2 shows a summary of the functional groups and new bonds provided by the corona treatment.

3.3 | Scanning electron microscopy

SEM micrographs of the biocomposites are shown in Figure 5, revealing clearly the individual layers. For all the treatments, it was observed a compact structure with few pores or cracks, but the joining region between the layers of the bilayer biocomposites was different according to the time of corona discharge applied. The transition between the layers is more evident and heterogeneous for the composite without the corona treatment (B0S), whereas the treatments with 60 and 90 s of discharge (B60S and B90S) showed an extremely homogeneous transition. It suggests that the treatment increased compatibility between layers, possibly by increasing hydrogen bond interactions among the film constituents at the interface, providing good adherence.[33] Figure 6 shows a schematic representation of the hydrogen bonding between the two layers.

3.4 | Tensile properties

Figure 7 presents the results obtained from the tensile tests (TS, TM, and E), conducted until the film ruptures. As observed in Figure 7A, the lamination process without corona discharge reduces tensile strength by 28%: TS for UNL was 10.2 MPa while for B0S it was 7.3 MPa. However, submitting the first layer film to 30 s of discharge

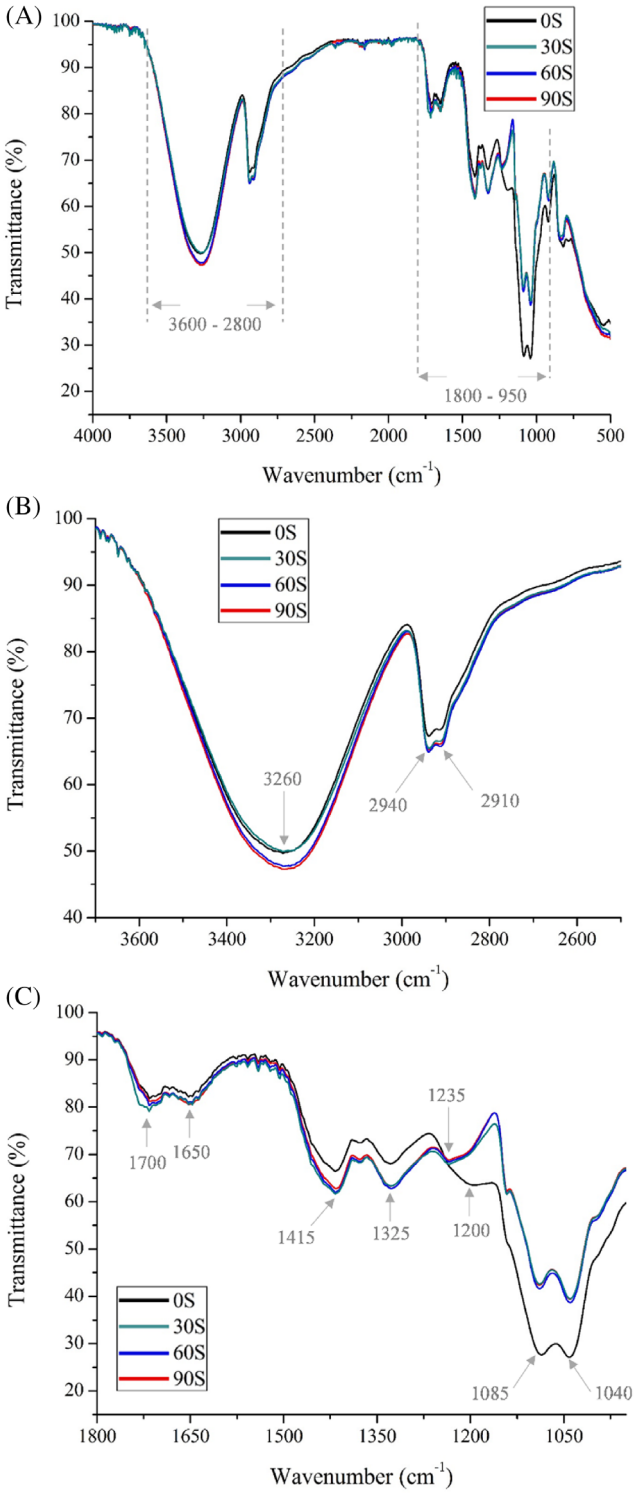

FIGURE 4 FT-IR spectra of the first layer films treated under different times of corona discharge (**A)** general spectra from 4000 cm^{-1} to 500 cm^{-1}; (**B)** range from 3600 cm^{-1} to 2800 cm^{-1}; and (**C)** range to 1800 cm^{-1} to 950 cm^{-1}

provided a slight increase in TS and, at 90 s of corona discharge, TS achieved 12.6 MPa, being 72% more resistant than B0S and 23% stronger than UNL film. Certainly, the good adherence between layers provided by corona treatment and predicted through water contact angle, surface energy, and SEM results, allowed this higher strength. This 12.6 MPa of tensile strength for B90S is a great tensile resistance value when compared, for example, with low-density polyethylene (LDPE), a material with widespread application in the food packaging sector, which presents (in different test conditions) TS of 6.9–16 MPa.[34,35]

TABLE 2 Summary of the functional groups and new bonds provided by the corona treatment

Wavenumber (cm^{-1})	Functional group
3260	–OH stretching
2940	asymmetrical stretching of $–CH_2$[14]
2910	symmetrical stretching of $–CH_2$[14]
1700 and 1650	axial deformation of –C=O and/or –O–C=O [32]
1415 and 1325	$–CH_3$ bending[30]
1235	formation of –C=O and/or –O–C=O [30,32]
1200	disappearance –C–O–C– stretching[30,32]
1085	reduction of –C–O– stretching[30,32]
1040	reduction –OH bending[30,32]

The tensile modulus of bilayer films was not affected by corona discharge at the periods of time used in this work (0, 30, 60, or 90 s), meaning that the treatment did not affect the films' rigidity. However, lamination provided films with 60% more flexibility when comparing the mean values of TM from B0S, B30S, B60S, and B90S with the TM result from UNL. Flexible food packaging widely used on the market, such as LDPE and linear LDPE (LLDPE), usually presents a tensile modulus varying between 130 and 300 MPa, which provides low stiffness and brittleness.[28,36,37] In this work, all bilayer films showed a mean TM of 28.6 MPa, being up to 9 times less rigid than these commercial polymers. Although different conditions of the test have been used in comparison with those commercial materials cited, the results here obtained can be extremely positive for some applications when super flexible and stretchable packaging is needed.[3]

de Oliveira, de Oliveira Begali, Ferreira, Ugucioni, de Sena Neto, Yoshida, and Borges,[5] when studying the effect of adding whey protein isolate to pectin packages, obtained values between 4.88 MPa and 6.30 MPa. Gomide et al.[38] obtained tensile strengths from 4.75 MPa to 6.43 MPa in whey protein isolate and lignin films. de Oliveira Begali, et al.[39] studied starch and pectin films and

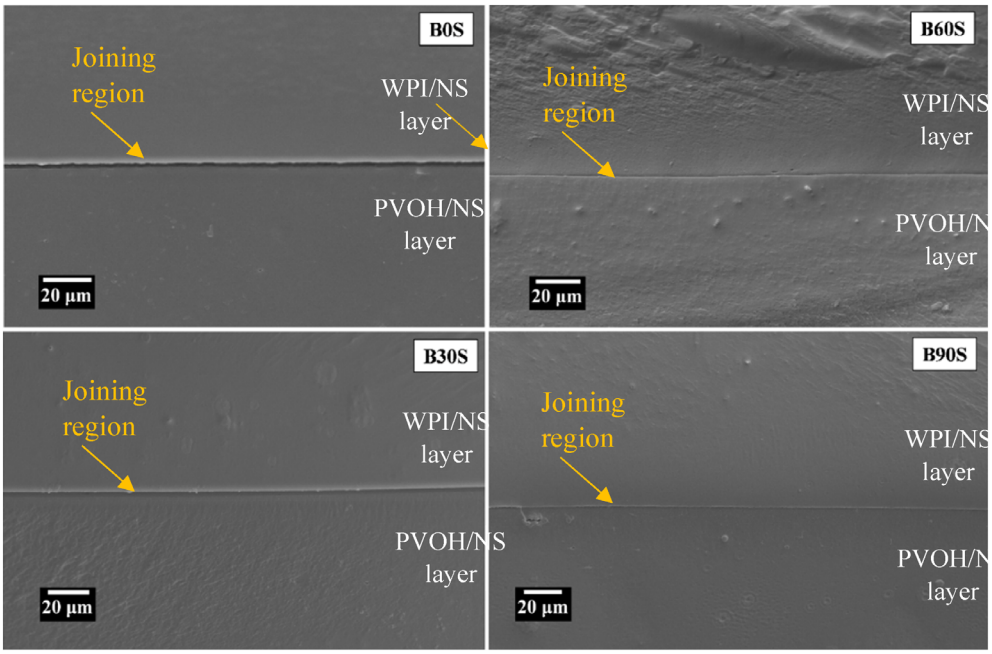

FIGURE 5 SEM cross-section micrographs showing the joining region between layers of the bilayer biocomposites: B0S, B30S, B60S, and B90S

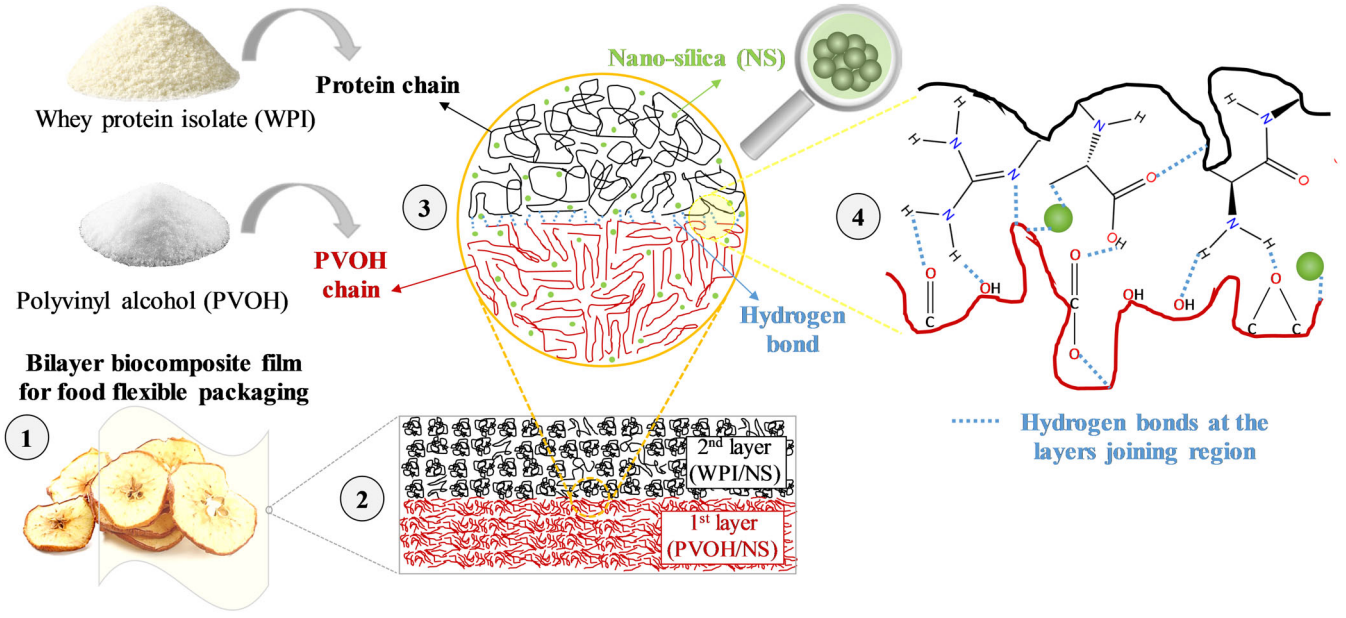

FIGURE 6 Schematic representation of the hydrogen bonding between the two layers

observed tensile strength values from 0.53 to 3.57 MPa. Thus, the tensile strength of these studies is greater than that found in previous studies, such as those mentioned.

By analyzing elongation results, it is possible to notice a behavior much more ductile for the film bilayer when compared to the unlaminated. Besides that, at 90 s of corona discharge, the treatment was able to provide a film 7.4 times more ductile when compared to UNL. Possibly, interactions between PVOH/PVOH chains and among film constituents on the first layer, and between WPI/WPI chains and among film constituents on the second layer, as well as interactions between layers, were more numerous when compared to interactions between all film constituents in a single phase on UNL film, allowing higher deformation before rupture.

These results corroborated the capacity of corona discharge in providing more polar groups available to interact between layers and among the film constituents, and that it is worth it to investigate composites and blends of different polymers not only in a single phase but also in separated phases using corona as an agent of adherence.

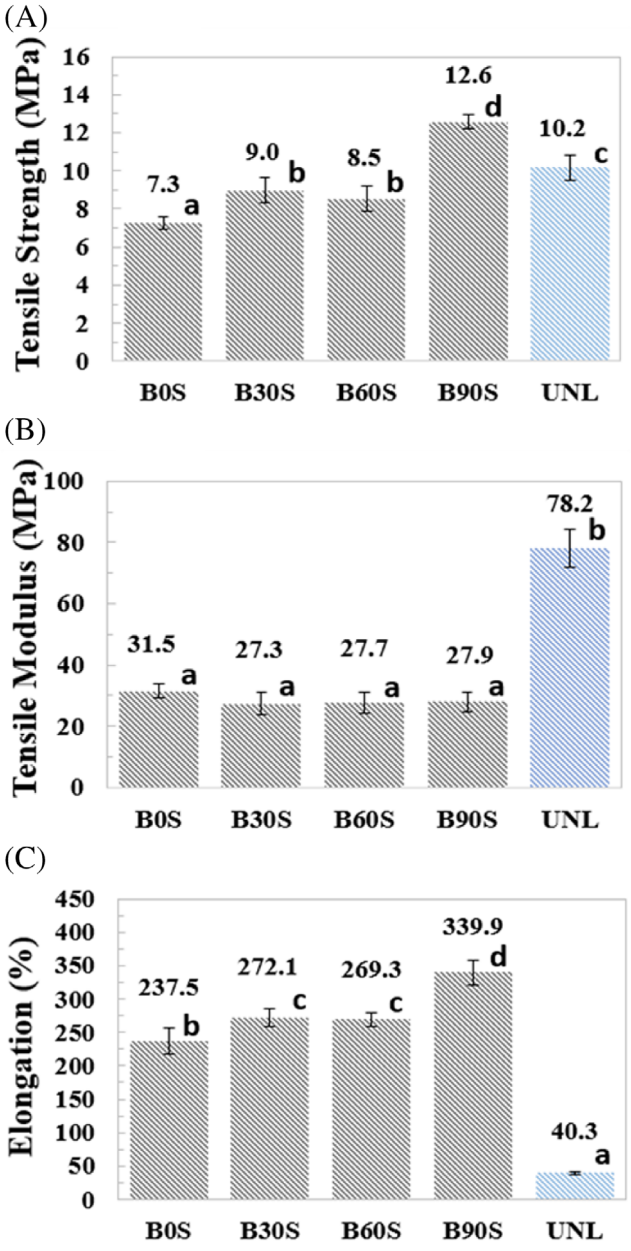

FIGURE 7 Average and standard deviation values of tensile properties (A) maximum TS and (B) TM and E were obtained by the tensile test of the biocomposites. Different letters represent significantly different values at ($p \geq .05$) using the Scott-Knott test.

3.5 | Water vapor permeability

The WVP test is essential for new materials intended to be applied as food packaging, such as the PVOH/WPI/NS bilayer biocomposites developed since it is important to know how the film will manage moisture ingress or regress. Intending to apply this film packaging to dry vegetables and fruits or cereals with a low water activity (a_w), the second layer of the film (WPI/NS) was chosen to be in contact with the interior of the capsule (a_w close to zero) in the water permeability test, and the second layer (PVOH/NS cross-linked with glutaraldehyde) to be the face in contact with the atmosphere (a_w of 0.75).[40] This way, we avoided food contact with possible traces of free glutaraldehyde and simulated similar conditions of the packaging inside and outside, respectively, with the inside and outside capsule environments. The permeability results (Table 3) showed that lamination, even without corona treatment, increased water permeability: B0S showed a P result 63.7% higher than the UNL film. Among bilayer films submitted to the corona discharge, there was no significant ($p \geq .05$) difference in P according to the times of discharge tested. Treatments with 30, 60, or 90 s of discharge, on average, showed water permeability 19.6% higher than that not treated (B0S) and 96% higher than the unlaminated film (UNL).

Since permeability takes both sorption and diffusion of water into consideration, it is important to evaluate coefficients of sorption and diffusion to better understand this rise in P when films were treated with corona discharge.

3.6 | Water diffusion and water solubility coefficients

The water diffusion and solubility coefficients obtained are shown in Table 3. The permeation of water vapor through a polymer sheet is related to both diffusivity and solubility, where the effective diffusion coefficient (D_{eff}) represents the speed of water molecules moving through the polymer matrix and the solubility coefficient (S) is related to the affinity of the matrix with water molecules, indicating the amount of water dissolved in the polymer.[28,29]

Lamination did not significantly ($p \geq .05$) change the diffusion coefficient, but lamination associated with corona treatment above 60 s acted decreasing D_{eff}. The B90S film showed a diffusion of 37% and 42% lower than those from B0S and UNL, respectively. Regarding the water solubility, it was increased by lamination and even more by corona discharge. At the 90s of discharge, the bilayer film had an S result 91% higher than that from the bilayer film without corona treatment (B0S) and 2.8 times higher than S from UNL. These results allow understanding of water permeability.

Water solubility is increased by corona treatment since the discharge raises the number of polar groups in the bilayer film matrix, as proved by FT-IR results, increasing, therefore, the affinity between the film and polar water molecules. This affinity acts by decreasing the speed of water permeating through the film, thus leading to lower values of D_{eff}. Despite this lower diffusion, observing the magnitude order of D_{eff} and S, it is

TABLE 3 Results of permeability coefficient (P), effective diffusion coefficient (D_{eff}), and solubility coefficient (S)

Biocomposite	Time of corona discharge (s)	Thickness (mm)	P (g.cm.cm^{-2}. s^{-1}. kPa^{-1}) × 10^{-10}	D_{eff} (cm^2. s^{-1}) × 10^{-6}	S (g.cm^{-3}. kPa^{-1}) × 10^{-5}
B0S	0	0.190 ± 0.02a	3.39 ± 0.09b	4.05 ± 0.28c	8.52 ± 0.82b
B30S	30	0.206 ± 0.01a	4.12 ± 0.42c	4.30 ± 0.16c	9.57 ± 0.94b
B60S	60	0.219 ± 0.02a	3.89 ± 0.33c	3.51 ± 0.26b	10.3 ± 1.23b
B90S	90	0.226 ± 0.02a	4.16 ± 0.36c	2.55 ± 0.29a	16.3 ± 0.72c
UNL	-	0.223 ± 0.01a	2.07 ± 0.24a	4.40 ± 0.41c	4.29 ± 0.15a

Note: In vertical columns, different letters represent significantly different values at ($p \geq 0.05$) using the Scott-Knott test.

possible to infer that solubility is more influential than diffusion in the water permeation process of the films tested. It indicates that corona treatment makes water pass slowly through the film but highly increases the affinity of this permeant with the matrix, making it more hygroscopic. Therefore, possibly, the lower water barrier (higher P) obtained for films treated with the discharge is related to higher water absorption at the film surface, and not a higher water vapor permeation through the film.

In terms of the lamination process, it was possible to conclude that PVOH/WPI in separated layers (B0S) favored a higher affinity of the film constituents with water molecules (raising S) when compared to the single-phase biocomposite (UNL). Therefore, despite the unchanged D_{eff} ($p \geq .05$), lamination decreased the water barrier.

4 | CONCLUSIONS

In the bilayer biocomposites, corona discharge increased the wettability of the first layer surface by generating new polar groups, improving the ability of the PVOH/NS surface to interact with the second layer of WPI/NS, thus increasing the adherence between these layers. Besides that, bilayer films treated with higher times (60 and 90 s) of discharge showed an extremely homogeneous transition between phases, suggesting compatibility and adherence between layers provided by the treatment. Bilayer films treated with 90 s of corona discharge showed a tensile strength of 72% and 23% more resistance than the bilayer film not treated and the single-layer film, respectively. Besides that, at 90 s of discharge, the bilayer film was 7.4 times more ductile when compared to the unlaminated one. Regarding the water barrier, the lamination process and corona treatment make water pass slowly through the film but increase the affinity of the water with the matrix, thus leading to a lower water barrier. Finally, the use of corona discharge associated with the lamination of PVOH/WPI/NS biocomposites providing a bilayer film is justified to produce a more resistant, flexible, and ductile biocomposite film for packaging.

ACKNOWLEDGMENTS

This work was financed by the Coordenação de Aperfeiçoamento de Pessoal de Nível Superior (CAPES)—Brasil (Finance Code 001), the Conselho Nacional de Desenvolvimento Científico e Tecnológico—Brasil (CNPq), and the Fundação de Amparo à Pesquisa do Estado de Minas Gerais—Brasil (FAPEMIG). The authors extend their appreciation for all the support provided by the Universidade Federal de Lavras (UFLA).

CONFLICT OF INTEREST

The authors declare no competing interest.

DATA AVAILABILITY STATEMENT

Data available on request from the authors.

ORCID

Bruna Rage Baldone Lara https://orcid.org/0000-0002-0700-7884

Ana Carolina Salgado de Oliveira https://orcid.org/0000-0003-1928-2856

REFERENCES

[1] S. Agarwal, *Eur. Polym. J.* **2021**, *160*, 110788.

[2] P. P. M. Size, *Share & Trends Analysis Report by Product (flexible, Rigid), by Technology (Extrusion, Thermoforming), by Application (Food & Beverages, Pharmaceuticals), and Segment Forecasts,* San Francisco **2021**, p. 2021. https://www.grandviewresearch.com/industryanalysis/plastic-packaging-market

[3] B. R. B. Lara, P. S. de Andrade, M. Guimarães Junior, M. V. Dias, L. A. P. Alcântara, *J. Polym. Environ.* **2021**, *29*(8), 2397.

[4] P. Oymaci, S. A. Altinkaya, *Food Hydrocoll.* **2016**, *54*, 1.

[5] A. C. S. de Oliveira, D. de Oliveira Begali, L. F. Ferreira, J. C. Ugucioni, A. R. de Sena Neto, M. I. Yoshida, S. V. Borges, *J. Food Process Eng.* **2021**, *44*, e13910.

[6] A. C. S. de Oliveira, J. C. Ugucioni, R. A. da Rocha, S. V. Borges, *J. Appl. Polym. Sci.* **2019**, *136*(14), 47316.

[7] S. Galus, J. Kadzińska, *Polym. Eng. Sci.* **2019**, *59*(S1), E375.

[8] B. R. B. Lara, A. C. M. A. Araújo, M. V. Dias, M. Guimarães, T. A. Santos, L. F. Ferreira, S. V. Borges, *Food Packag. Shelf Life* **2019**, *19*, 16.
[9] X. Chen, F. Cui, H. Zi, Y. Zhou, H. Liu, J. Xiao, *Int. J. Biol. Macromol.* **2019**, *141*, 1175.
[10] B. Das, D. Chakrabarty, C. Guha, S. Bose, *Polym. Eng. Sci.* **2021**, *61*(5), 1449.
[11] A. Popelka, I. Novák, M. A. S. A. Al-Maadeed, M. Ouederni, I. Krupa, *Surf. Coat. Technol.* **2018**, *335*, 118.
[12] T. A. Lopes, L. Bufalino, P. I. C. Claro, M. A. Martins, G. H. D. Tonoli, L. M. Mendes, *Cellulose* **2018**, *25*(9), 5017.
[13] R. V. Gadhave, P. A. Mahanwar, P. T. Gadekar, *Des. Monomers Polym.* **2019**, *22*(1), 164.
[14] K. C. S. Figueiredo, T. L. M. Alves, C. P. Borges, *J. Appl. Polym. Sci.* **2009**, *111*(6), 3074.
[15] K. M. Albano, Â. L. F. Cavallieri, V. R. Nicoletti, *Food Rev. Int.* **2019**, *35*(1), 54.
[16] R. Andrade, O. Skurtys, F. Osorio, R. Zuluaga, P. Gañán, C. Castro, *LWT—Food Sci. Technol.* **2014**, *58*(1), 158.
[17] S. Farris, L. Introzzi, P. Biagioni, T. Holz, A. Schiraldi, L. Piergiovanni, *Langmuir* **2011**, *27*(12), 7563.
[18] T. Karbowiak, F. Debeaufort, A. Voilley, *Crit. Rev. Food Sci. Nutr.* **2006**, *46*(5), 391.
[19] M. Kurek, S. Galus, F. Debeaufort, *Food Packag. Shelf Life* **2014**, *1*(1), 56.
[20] A. E. Wiącek, *Food Hydrocoll.* **2015**, *48*, 228.
[21] Y.-C. Yin, S.-W. Yin, X.-Q. Yang, C.-H. Tang, S.-H. Wen, Z. Chen, B.-j. Xiao, L.-Y. Wu, *Food Hydrocoll.* **2014**, *36*, 1.
[22] A. S. Ferreira, C. Nunes, A. Castro, P. Ferreira, M. A. Coimbra, *Carbohydr. Polym.* **2014**, *113*, 490.
[23] A. S. F. Testing, D–08, M.*Standard Practice for Surface Wettability of Coatings, Substrates And Pigments by Advancing Contact Angle Measurement*, ASTM International, West Conshohocken **2013**.
[24] D. K. Owens, R. C. Wendt, *J. Appl. Polym. Sci.* **1969**, *13*(8), 1741.
[25] ASTM-D882, *Standard Test Methods for Tensile, Properties of Thin Plastic Sheeting*, West Conshohocken **2002**.
[26] *ASTM-E96/E96M, E96/E96M-16 Standard Test Methods for Water Vapor Transmission of Materials,* West Conshohocken **2016**.
[27] J. Crank, *The Mathematics of Diffusion*, In Clarendon Press, Oxford **1975**, p. 414.
[28] G. L. Robertson, *Food Packaging: Principles and Practice*, CRC Press, Boca Raton **2005**.
[29] Janjarasskul, T.; Tananuwong, K., *Role of Whey Proteins in Food Packaging*. Elsevier, Amsterdam, Netherlands **2019**.
[30] J. R. Rocca-Smith, T. Karbowiak, E. Marcuzzo, A. Sensidoni, F. Piasente, D. Champion, O. Heinz, P. Vitry, E. Bourillot, E. Lesniewska, *Polym. Degrad. Stab.* **2016**, *132*, 109.
[31] L. Dai, D. Xu, *Tetrahedron Lett.* **2019**, *60*(14), 1005.
[32] V. C. Louzi, J. S. D. C. Campos, *Surf. Interfaces* **2019**, *14*, 98.
[33] J. F. Martucci, R. A. Ruseckaite, *J. Food Eng.* **2010**, *99*(3), 377.
[34] H. F. Mark, N. M. Bikales, C. G. Overberger, G. Menges, *Encyclopedia of Polymer Science and Engineering*, Vol. 4, Wiley-Interscience, 605 Third Avenue, New York, New York, USA **1986**, 10158.
[35] A. Shebani, A. Klash, R. Elhabishi, S. Abdsalam, H. Elbreki, W. Elhrari, *Res. Dev. Mater. Sci.* **2018**, *7*(5), 791.
[36] T. Jin-hua, L. Guo-qin, C. Huang, S. Lin-jian, *Mater. Res.* **2012**, *15*, 1050.
[37] S. Selke, R. Hernandez, *Encyclopedia of Materials: Science and Technology*, Oxford **2011**, p. 6652.
[38] R. A. C. Gomide, A. C. S. de Oliveira, L. B. Luvizaro, M. I. Yoshida, C. R. de Oliveira, S. Borges, *J. Food Process. Eng.* **2020**, *44*, e13596.
[39] D. de Oliveira Begali, L. F. Ferreira, A. C. S. de Oliveira, S. V. Borges, A. R. de Sena Neto, C. R. de Oliveira, M. I. Yoshida, C. I. G. L. Sarantopoulos, *Int. J. Biol. Macromol.* **2021**, *180*, 262.
[40] B. R. B. Lara, M. V. Dias, M. Guimarães Junior, P. S. de Andrade, B. de Souza Nascimento, L. F. Ferreira, M. I. Yoshida, *Food Hydrocoll.* **2020**, *103*, 105710.

SUPPORTING INFORMATION

Additional supporting information can be found online in the Supporting Information section at the end of this article.

How to cite this article: B. R. B. Lara, P. S. de Andrade, A. C. S. de Oliveira, M. G. Junior, L. C. Matos, G. H. D. Tonoli, M. V. Dias, *Polym. Eng. Sci.* **2022**, *62*(12), 3923. https://doi.org/10.1002/pen.26150